

See discussions, stats, and author profiles for this publication at: <https://www.researchgate.net/publication/284799440>

# A compact very wideband amplifying filter based on RTD loaded composite right/left-handed transmission lines

Article in SpringerPlus · December 2015

DOI: 10.1186/s40064-015-1529-y

CITATIONS

0

READS

87

2 authors, including:



H. J. El-Khozondar  
Islamic University of Gaza

88 PUBLICATIONS 358 CITATIONS

[SEE PROFILE](#)

Some of the authors of this publication are also working on these related projects:



Slab waveguide as a sensor [View project](#)



Use computer simulations based on Monte Carlo Potts model to study the topological features of Ostwal ripening in two-phase polycrystalline materials [View project](#)



This article appeared in a journal published by Elsevier. The attached copy is furnished to the author for internal non-commercial research and education use, including for instruction at the authors institution and sharing with colleagues.

Other uses, including reproduction and distribution, or selling or licensing copies, or posting to personal, institutional or third party websites are prohibited.

In most cases authors are permitted to post their version of the article (e.g. in Word or Tex form) to their personal website or institutional repository. Authors requiring further information regarding Elsevier's archiving and manuscript policies are encouraged to visit:

<http://www.elsevier.com/authorsrights>



Contents lists available at ScienceDirect

Optik

journal homepage: [www.elsevier.de/ijleo](http://www.elsevier.de/ijleo)

## Nonlinear resonant tunneling diode (RTD) circuits for microwave A/D conversion



Hala J. El-Khozondar<sup>a,\*</sup>, Rifa J. El-Khozondra<sup>b</sup>, Ahmed R.S. AL-Farra<sup>a</sup>, Bernard Z. Essimbi<sup>c</sup>

<sup>a</sup> Electrical Engineering Department, Islamic University of Gaza, P.O. Box 108, Palestine

<sup>b</sup> Physics Department, Al-Aqsa University, P.O. Box 4051, Palestine

<sup>c</sup> ZHO, Optoelectronics, University of Duisburg-Essen, D-47048 Duisburg, Germany

### ARTICLE INFO

#### Article history:

Received 3 December 2012

Accepted 28 April 2013

#### Keywords:

Solitons

Nonlinear transmission lines

Resonant tunneling diodes

Analog to digital conversion

### ABSTRACT

Short-duration electrical pulses play important roles in ultrafast time-domain metrology: they are used to sample rapidly varying signals or as probe signals in ranging radars, time-domain reflectometry and in communication. In this work, we design a nonlinear transmission, which is loaded with resonant tunneling diode to be suitable for microwave A/D conversion. A resonant tunneling diode (RTD) has a negative differential resistance that means when the voltage increases the current decreases. The equivalent circuit of monostable line is given. The simulation is performed by using OrCad program. Results show that a spike is produced and after a charging time constant, another switching occurs. Hence – similar to a relaxation oscillator – the spiking period is determined by the amplitude and frequency of the input current. The transmission line itself ensures the generation and propagation of identical spikes, such as solitons formed after few diodes.

© 2013 Elsevier GmbH. All rights reserved.

### 1. Introduction

The importance of nonlinear transmission lines (NLTs) in microwave engineering has attracted considerable attention [1–3]. NLTs consisting of coplanar waveguide (CPW) can generate picosecond electrical pulses [4]. Among the very large number of guiding structures proposed and used in microwave applications, planar waveguides have proved an interest for monolithic microwave integrated circuits (MMICs). Moreover, NLTs are convenient analog devices to simulate the nonlinearity of physical systems as for example a physical phenomenon noticed for gap solitons in electrical superlattices [5]. NLTs are developed as the main components for millimeter wave generation and processing [6]. These NLTs have practical applications in a variety of high speed, wide bandwidth systems comprising picosecond resolution sampling circuits and millimeter wave sources [7]. Essimbi and Jaeger [8] proposed a method of generating electrical short pulses on a Schottky transmission line periodically loaded with resonant tunneling diodes. RTD-NLTL can provide the basis of very interesting microwave signal generation and processing circuits such as an oscillator or an A/D converter [3].

RTDs first proposed by Chang et al. [9] have attracted much attention for various circuit applications. RTDs are currently the widest bandwidth active semiconductor devices. They have an estimated maximum frequency of 2.2 THz against 215 GHz in conventional Complementary Metal Oxide Semiconductor transistors [10]. RTDs have shown promising circuit characteristics in improving both analog and digital circuits, due to their high switching speed capability and multipurpose functionality. For example, numerous RTD-based circuits have been described working at clock frequencies of GHz, including the basic logic gates [11], flip-flops [12], analog-to-digital convertor (ADC) [13], amplifiers [14], and oscillators [15]. The characteristic of the RTD is a nonlinear N-shaped current voltage relationship giving active behavior at millimeter wave frequencies.

The focus of this study is on RTD-NLTL analog-to-digital converters (ADC's), which have applications in sampling scopes, digital receivers, and phased array radars [16,17]. Essimbi and Jaeger [13] suggested a way for producing short electrical pulses by means of Schottky periodically integrating RTD. Jaeger et al. [18] showed that NLTs consisting of a periodic array of RTDs in a coplanar waveguide (RTD-NLTL) can be used as a millimeter wave oscillator. The paper is introduced a novel way to get ADC by using NLTs loaded with RTD. The frequency and amplitude of the input signal is changed to study its effect on the output of the transmission line using OrCad simulation program. The paper is organized as follows: theoretical background of the RTD-NLTL is covered in Section 2. In Section 3,

\* Corresponding author. Tel.: +972 82860700; fax: +972 82860800.

E-mail addresses: [hkhonzondar@iugaza.edu](mailto:hkhonzondar@iugaza.edu) (H.J. El-Khozondar), [rifa20012002@yahoo.com](mailto:rifa20012002@yahoo.com) (R.J. El-Khozondra).

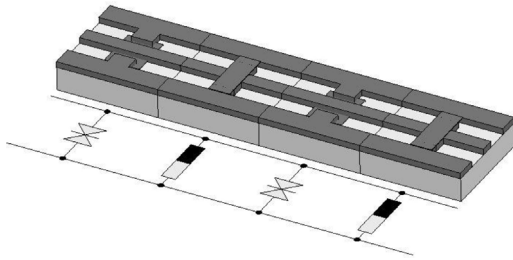


Fig. 1. Sketch of an RTD-NLTL using a coplanar transmission line.

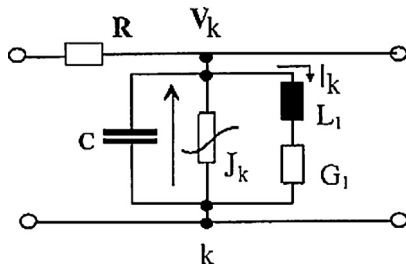


Fig. 2. Schematic representation of the  $n$ th section of RTD-NLTL.

the analysis performed using OrCad is given. Conclusion is followed in Section 4.

### 2. Theoretical background of the RTD-NLTLs

A schematic sketch of the RTD-NLTL is displayed in Fig. 1. The RTD-NLTL is a coplanar transmission line periodically loaded with RTDs. Fig. 2 shows the equivalent circuit of the  $n$ th section of the RTD-NLTL. Each section encompasses a T-shape piece corresponding to the transmission line. It consists of a series resistance  $R$  and a shunt conductance–capacitance ( $J_k(V_k) - C$ ) circuit, the active section of RTD, in parallel with a series inductance–conductance ( $L_1, G_1$ ) circuit. The output port of the coplanar transmission line is set free. In this case we do not have to worry about reflection effect and oscillation effects. The nonlinearity is found by using the characteristic current–voltage relationship given by

$$J_k(V) = BV_k(V_k - U_1)(V_k - U_2), \quad (1)$$

where an external bias current is applied,  $U_1, U_2$  are voltages which determine the zeros of  $J_k$  and  $B$  is an amplitude factor determined by the slope at  $V=0$ . In this work, we supposed  $U_1, U_2 > 0$ .

The nonlinear current–voltage characteristic curve created by OrCad is illustrated in Fig. 3. In Fig. 3,  $S_1$  and  $S_2$  represent positive and negative areas for  $J(V)$  characteristics. The area constraints on pulse growth during propagation along the line are as follows [8]: in the region,  $S_1 > S_2$ , the pulse shrinks; for  $S_1 < S_2$ , the pulse grows, and when  $S_1 = S_2$ , the pulse length remains unchanged.

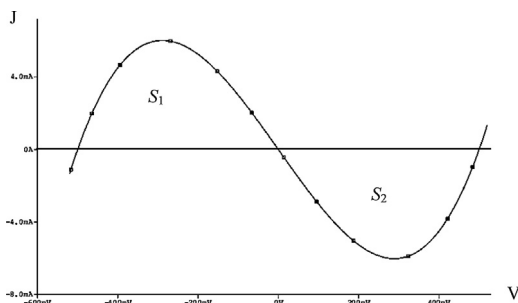


Fig. 3. Current–voltage characteristic curve of RTD where  $S_1 = S_2$ .

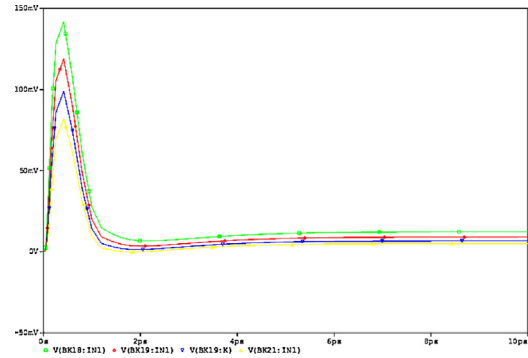


Fig. 4. The output pulse of an input rectangular pulse with amplitude 2.5 V and pulse duration 40 ps at  $k=18$  (green),  $k=19$  (red),  $k=20$  (blue) and  $k=21$  (yellow). (For interpretation of the references to color in this figure legend, the reader is referred to the web version of this article.)

Applying Kirchhoff's voltage law, the voltage across the inductance  $L_1$  is

$$L_1 \frac{dI_k}{dt} = V_k - \frac{I_k}{G_1}, \quad (2)$$

and using Kirchhoff's current law, the current passing through  $C_1$

$$C \frac{dV_k}{dt} = \frac{1}{R}(V_{k-1} - 2V_k + V_{k+1}) - J_k - I_k \quad (3)$$

where  $V_k, I_k$  are the voltages at element  $k$  and the resulting current through the series inductance–conductance ( $L_1, G_1$ ) circuit, respectively.

### 3. Numerical analysis

We have used a computer OrCad program to study the RTD-NLTL. All numerical parameters are taken from the experimental values given by [13]. The proposed RTD-NLTL is composed of  $N=40$  identical segments, resistively attached to linear resistor having the value,  $R=0.5 \Omega$ . The electrical parameters of each segment are  $B=1 \text{ A V}^{-3}$ ,  $C=0.01 \text{ pF}$ ,  $L_1=10 \text{ pH}$ ,  $R_1=1/G_1=5 \Omega$ . Initial rectangular pulses as well as a sinusoidal input signal are launched into the network to study freely propagating waves. Furthermore, we considered two cases for every input signal: case 1 for  $S_1/S_2 > 1$  and case 2 for  $S_1/S_2 < 1$ .

#### 3.1. Rectangular input signal: case 1 for $S_1/S_2 > 1$

The values of  $U_1=0.35 \text{ V}$  and  $U_2=0.5 \text{ V}$  are chosen such that  $S_1/S_2 > 1$ . Fig. 4 shows the numerical results for an initial input square signal with amplitude of magnitude equal to 2.5 V and pulse duration of value equal to 40 ps. The output is taken for elements from  $k=18$  to  $k=21$ . It is clear that the output is one signal with amplitude vanishing along the line. This means that the effect of  $J(V)$  is dissipative.

#### 3.2. Rectangular input signal: case 2 for $S_1/S_2 < 1$

We have taken an input rectangular signal with amplitude 1 V and pulse duration 50 ps for  $U_1=0.2$  and  $U_2=1$  which implies that  $S_1/S_2 < 1$ . Fig. 5 demonstrates the numerical results at element  $k=21$ . The red line indicates for the input signal and the blue line indicates for the output signal. It is clear that the output of the RTD-NLTL contains 9 pulses. Following, the value of the amplitude of initial rectangular pulse stayed constant (1 V) and the value of its pulse duration is changed to 40 ps. Numerical results at element  $k=21$  are exhibited in Fig. 6. The input signal is represented by red lines and the output is represented by blue lines. It is shown that the

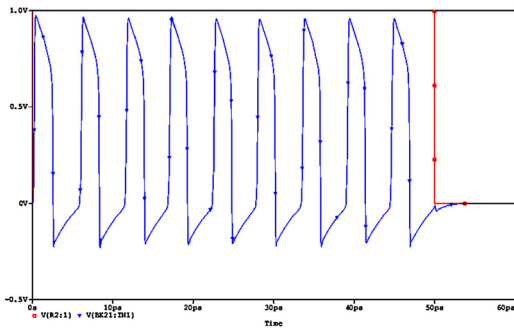


**Fig. 5.** The output 9 pulses at element  $k=21$  (blue) for input rectangular pulse with amplitude 1 V and pulse duration 50 ps (red). (For interpretation of the references to color in this figure legend, the reader is referred to the web version of this article.)

RTD-NLTL produce output signal consists of 7 pulses. Next, for the same frequency of the rectangular input signal (40 ps), we changed the amplitude value to 5 V. We observed from Fig. 7 the appearance of 8 pulses generated at element  $k=21$ . The blue line refers to the output pulses and the red line refers to the input rectangular pulse. We notice that the number of pulses depends on the characteristic parameters of the input signal; the number of pulses is altered in a characteristic way. This implies that for the case  $(S_1/S_2) < 1$ , the system acts as a source of energy so that losses are rewarded by magnification along the network.

### 3.3. Sinusoidal input signal: case $S_1/S_2 < 1$

In this case, we apply sinusoidal signal at the input of the RTD-NLTL with frequency of 10 GHz and amplitude of 5 V. The output at element  $k=18$  (green line) is illustrated in Fig. 8. The input signal is represented by red line. We see a group of 8 pulses appearing only in the positive part of the input signal.

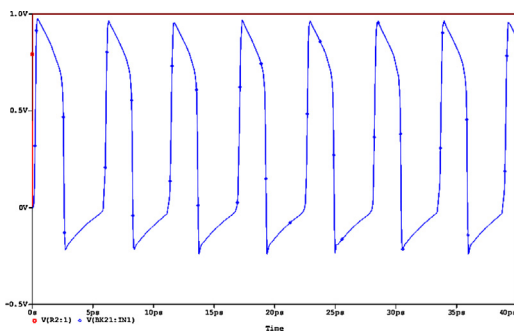


**Fig. 6.** The output 7 pulses at element  $k=21$  (blue) for input rectangular pulse with amplitude 1 V and pulse duration 40 ps (red). (For interpretation of the references to color in this figure legend, the reader is referred to the web version of this article.)

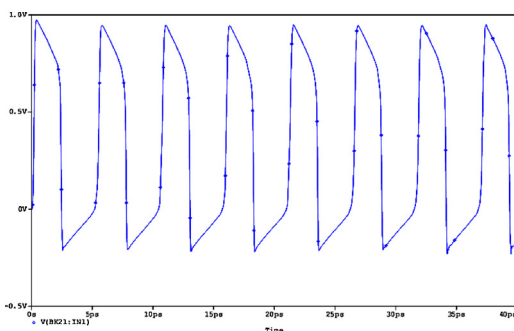


**Fig. 7.** The output 8 pulses at element  $k=21$  for input rectangular pulse with amplitude 5 V and pulse duration 40 ps.

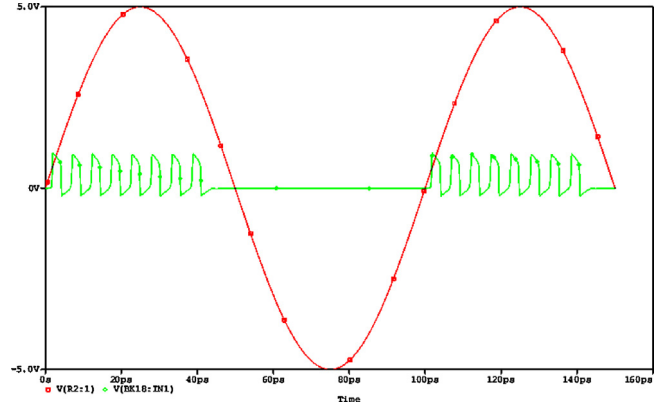


**Fig. 8.** The output 8 pulses per period at element  $k=18$  for input sinusoidal pulse with amplitude 5 V and frequency 10 GHz.

Additionally, the duration of the input sinusoidal signal remained constant 10 GHz and the amplitude of the sinusoidal wave is changed to 2 V. The output at element  $k=18$  is shown in Fig. 9. We notice from Fig. 9 that we can get a set of 7 pulses appearing in the positive part of the input signal.

Further, for the same amplitude 2 V, we set the frequency to 20 GHz. Fig. 10 exhibits that the output at  $k=18$  is a set of 4 pulses in the positive part of the input signal. Fig. 11 exhibits the output of a sinusoidal signal with amplitude 5 V and frequency 20 GHz. The output exhibits 4 pulses in the positive part of the input signal.

Fig. 12 demonstrates the output at element  $k=18$  for input sinusoidal signal with amplitude 2 V and frequency 50 GHz. The output is a collection of 2 pulses in the positive part of the input signal. However, the collection of the 2 pulses does not have a fixed pulse shape. Next, for the same frequency 50 GHz, we changed the value of the amplitude to 5 V. The numerical results at element  $k=18$  are shown in Fig. 13. We see from Fig. 13 that we can get a cluster

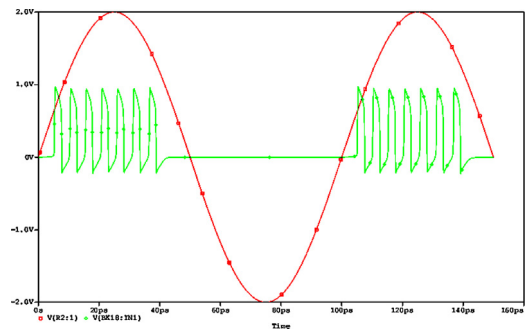


**Fig. 9.** The output 7 pulses at  $k=18$  for input sinusoidal pulse with amplitude 2 V and frequency 10 GHz.

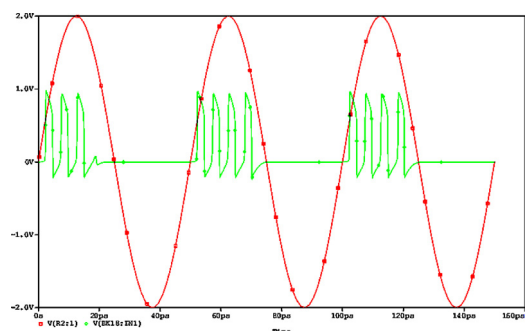


**Fig. 10.** The output 4 pulses at  $k=18$  for input sinusoidal pulse with amplitude 2 V and frequency 20 GHz.



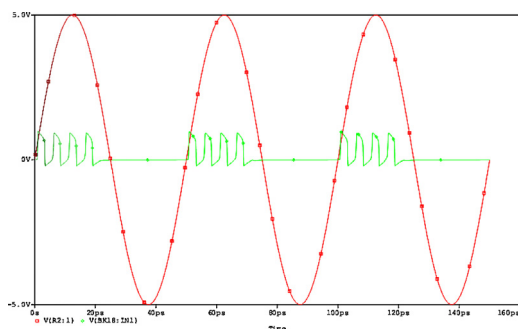


**Fig. 11.** The output 4 pulses at  $k = 18$  for input sinusoidal pulse with amplitude 5 V and frequency 20 GHz.

of 2 pulses which maintain their shape as they propagate along the NLTL. The output of 5 V amplitude sinusoidal with frequency 100 GHz at element 18 is shown in Fig. 14. Fig. 14 shows a single train of output pulse in the positive part of the input signal. Thus, it is obvious that the number of the pulses changes as the characteristics of the input signal is changed.

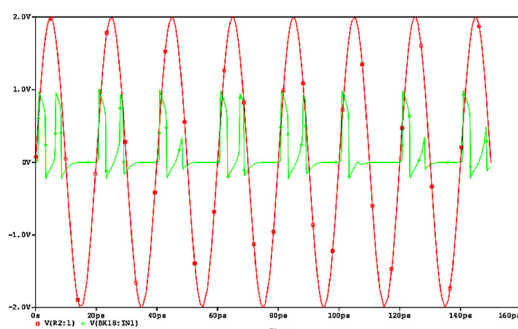


**Fig. 12.** The output 2 pulses at  $k = 18$  for input sinusoidal pulse with amplitude 2 V and frequency 50 GHz.

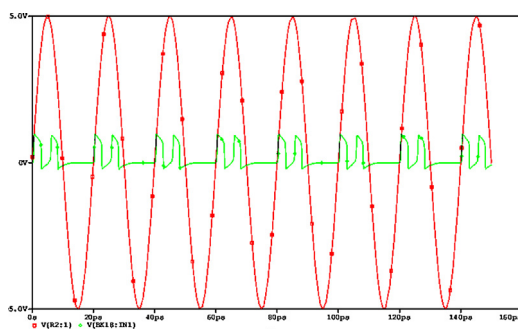


**Fig. 13.** The output 2 pulses at  $k = 18$  for input sinusoidal pulse with amplitude 5 V and frequency 50 GHz.

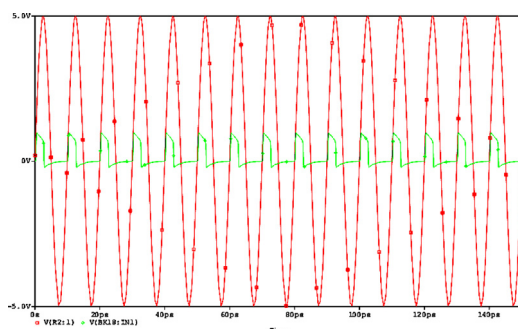


**Fig. 14.** The output 1 pulses at  $k = 18$  for input sinusoidal pulse with amplitude 5 V and frequency 100 GHz.

#### 4. Discussion and Conclusion

The OrCad analysis agrees with the previous study [13]. In this study, we examined the effect of changing frequency of the input signal on the output spikes number and position. From the previous circuit analysis, we deduce that the circuit source is roughly the following. An input current source charges the capacitance  $C$  up to a threshold value given by  $J(V)$  of the RTD. Therefore, a switching up occurs which will be inverted due to the LG time constant (inductor-conductance effect). As a result, a spike is produced and after RC time constant (capacitor-resistor effect) another switching occurs. Hence the spiking period is determined by the amplitude of the input current. When the input frequency or the input amplitude is changed, the number, phase, and position of the spikes are altered in a characteristic way. However, we noticed that the effect of frequency is more than the effect of the amplitude.

In conclusion a novel monostable RTD-NLTL in MMIC technology is proposed which can generate characteristic pulse pattern for a given input signal. That is the position and number of spikes at the output depends on the input signal amplitude and frequency. We used OrCad program to analyze the proposed RTD-NLTL for millimeter-wave sources. We got collections of pulses at the output frequencies up to 0.1 THz. These NLTLs can be used to realize an ultra-fast  $n$ -bit A/D converter. Thus we propose common  $n$ -channel (for  $n$  bits) coplanar signal divider to provide input amplitudes by power of 2. Hence each channel delivers a spike train to the output array establishing a Gray code.

#### References

- [1] K. Narahara, T. Otsuji, E. Sano, Generation of electrical short pulse using Schottky line periodically loaded with electronic switches, *J. Appl. Phys.* 100 (2006) 24511–24515.
- [2] D. Ricketts, X. Li, N. Sun, K. Woo, D. Ham, On the self-generation of electrical soliton pulses, *IEEE J. Solid-State Circ.* 42 (2007) 1657–1668.
- [3] H. El-Khozondar, R. El-Khozondar, I. Abo Ireban, *Transmission Lines and Schottky Diode: Nonlinear Transmission Lines*, LAP Lambert Academic Publishing, Germany, 2011.
- [4] M. Remoissenet, *Waves Called Solitons. Concepts and Experiments*, Springer, Berlin, 1999, pp. 37–64.
- [5] J.M. Bilbault, M. Remoissenet, Gap solitons in nonlinear electrical superlattices, *J. Appl. Phys.* 70 (1991) 4544–4550.
- [6] J. Robinson, Y. Rahmat-Samii, Particle swarm optimization in electromagnetics, *IEEE Trans. Ant. Propagat.* 52 (2004) 397–407.
- [7] M.J. Rodwell, S.T. Allen, R.Y. Yu, M.G. Cas, U. Bhattacharya, M. Reddy, E. Carman, M. Kamegawa, Y. Konishi, J. Puhl, R. Pallela, Active nonlinear wave propagation devices in ultrafast electronics and optoelectronics, *Proc. IEEE* 82 (1994) 1037–1059.
- [8] B.Z. Essimbi, D. Jaeger, Generation of electrical short pulses using a Schottky transmission line periodically loaded with tunnelling diodes, *Curr. Appl. Phys.* 5 (2005) 567–571.
- [9] L.L. Chang, L. Tsu, T. Esaki, Resonant tunnelling in semiconductor double barriers, *Appl. Phys. Lett.* 24 (1974) 593–595.
- [10] S.T. Allen, *Schottky diode integrated circuits for sub-millimeter-wave applications*, University of California, Santa Barbara, 1994 (Ph.D. Thesis).
- [11] W. Williamson, S.B. Enquist, D.H. Chow, H.L. Dunlap, S. Subramaniam, P. Lei, G.H. Bernstein, B.K. Gilbert, 12 GHz clocked operation of ultralow power interband resonant tunneling diode pipelined logic gates, *IEEE J. Solid-State Circ.* 32 (1997) 222–231.
- [12] H. Matsuzaki, T. Itoh, M. Yamamoto, A novel high-speed flip-flop circuit using RTDs and HEMTs, *Proc. Great Lake Symp. LSI I* (1999) 154–157.
- [13] B.Z. Essimbi, D. Jaeger, Electrical short pulses generation using a resonant tunneling diode nonlinear transmission line, *Phys. Scr.* 85 (2012) 1–5.
- [14] R.F. Trambaruo, Esaki diode amplifiers at 7, 11 and 26 kMc/s, *Proc. IRE* 48 (1960) 2022–2023.
- [15] D. Ricketts, X. Li, D. Ham, Electrical soliton oscillator, *IEEE Trans. Microwave Theory Tech.* 54 (2006) 373–382.
- [16] K. Poulton, K.L. Knudsen, J. Kerley, Kang, J. Tani, E. Cornish, M. VanGrouw, An 8 GSa/s 8-bit ADC system, *Proc. Symp. VLSI Circ. Tech. Dig. 1* (1997) 23–24.
- [17] P. Xiao, K. Jenkins, M. Soyuer, H. Ainspan, J. Burghartz, H. Shin, M. Dolan, D. Harame, A 4 b 8 G Sample/s A/D converter in SiGe bipolar technology, *IEEE Int. Solid-State Circ.* 124–125 (1997).
- [18] I. Jaeger, D. Kalinowski, A. Stöhr, A. Stiens, R. Vounckx, D. Jäger, Millimetre wave signal generation using resonant tunneling diodes NLTL resonators, *Microwave Opt. Technol. Lett.* 29 (2007) 2907–2909.